*Proceedings of the 8th World Congress on Momentum, Heat and Mass Transfer (MHMT'23)*
*Lisbon, Portugal – March 26 – 28, 2023*
*Paper No. CSP 109*
*DOI: 10.11159/csp23.109*

# Insights into Multi-Stage Heat Release Phenomenon of Polyoxymethylene Dimethyl Ether 1 ($PODE_1$)

**Denis Buntin[1], Leonid Tartakovsky[1, 2]**
[1] Faculty of Mechanical Engineering, Technion – Israel Institute of Technology
Technion City, Haifa 3200003, IL, Israel
buntin@campus.technion.ac.il; tartak@me.technion.ac.il
[2] Grand Technion Energy Program, Technion – Israel Institute of Technology
Technion City, Haifa 3200003, IL, Israel

***Abstract*** **-** Transition to sustainable energy origins, carbon-neutral energy carriers and leaner-burning combustion concepts is strongly discussed for its prospective role in greener and secure energy future. Polyoxymethylene dimethyl ethers ($PODE_n$), well-suited for compression-ignition combustion modes, are considered as potential carbon-neutral candidates. To elucidate their potential, a detailed knowledge of *lean* $PODE_n$ combustion characteristics, as well as underlying chemical kinetics, is necessary. In this paper, numerical insights into multi-stage heat release peculiarities of $PODE_1$/oxidizer propellant pertinent to lean spontaneous auto-ignition, are presented and compared to n-heptane. Macro-dynamics of *three-stage heat release (3SHR) phenomenon*, earlier revealed by the authors to predominantly occur at low-to-intermediate initial temperatures (below 900 K) at ultra-lean conditions (equivalence ratios ($\varphi$) below 0.5), is discussed. For this task, *initial-state sensitivity analysis* of the heat release rate (HRR) characteristic parameters (e.g., peak amplitudes, proximities), was conducted. Detailed $PODE_1$ kinetic mechanisms, formerly identified as the most accurate for lean $PODE_1$ autoignition, were utilized for constant-volume adiabatic reactor simulations at initial temperatures of 600-900 K, pressures of 10-40 bar, and $\varphi$ = 0.1-0.5. Results revealed distinct perturbing effects of initial-state parameters on 3SHR macro-dynamics, sensed through raw and logarithmic derivative profiles of peak proximities and amplitudes. $PODE_1$ and n-heptane showed several contrary results attributed to dissimilarities in negative temperature coefficient (NTC) behavior.

***Keywords*****:** $PODE_1$, methylal, multi-stage heat release, auto-ignition, chemical kinetics

## 1. Introduction

Polyoxymethylene dimethyl ethers ($CH_3O(CH_2O)_nCH_3$, $PODE_n$, $OME_n$) are intensively discussed as promising low-emission/carbon-neutral synthetic alternatives for compression-ignition (CI) based systems. $PODE_n$ are highly reactive non-toxic compounds (cetane number (CN) ≥63, n>1), featured by comparatively low C/H ratios, high O-content, and no C-C bonds. The latter result in reduced soot precursors formation, and thus in decreased particulate-matter (PM) emissions. To reduce the net $CO_2$ emissions, $PODE_n$ can be renewably produced through $CO_2$ capturing (thus referred to as e-fuels) [1–3]. The simplest representative of $PODE_n$ family is $PODE_1$ ($CH_3O(CH_2O)_{n=1}CH_3$, dimethoxymethane (DMM) or methylal). Compared to dimethyl ether (DME), $PODE_1$ is liquid at ambient conditions (BP=42°C), has higher oxygen content (42.1 wt.%), lower vapor pressure, and better solubility in diesel fuel. $PODE_1$ accounts for the highest, among $PODE_n$, heating value (22.4 MJ/kg), yet the lowest CN (29, 38), lower than DME (CN=55) or neat diesel fuel (CN=45-52). Research in CI engines has shown that adding $PODE_1$ and/or higher-order $PODE_n$ to diesel fuel results in particle emission reduction and engine efficiency increase, positively affecting $NO_x$/PM tradeoff [4–6].

Auto-ignition (AI) study is crucial for modern CI-based propulsion (e.g., Homogeneous-Charge-CI (HCCI) [7], Reactivity-Controlled-CI (RCCI) engines [8], etc.). The current work extends our former numerical study [9] on the multi-stage (i.e., two-/three-stage) heat release of lean-to-rich AI of $PODE_1$/air mixtures. A widened scope of macro (i.e., global) AI-characteristics (compared to n-heptane) of *unusual three-stage heat release (3SHR) phenomenon* [9] (e.g., Fig 1), prevalent in *ultra-lean* AI, is examined. This work improves our understanding of *macro-dynamics* of $PODE_1$-3SHR in AI regimes, subjected to thermal and chemical feedback.

## 2. Computation and modeling methods

Similarly to preceding study [9], PODE$_1$/air combustion was simulated in CHEMKIN-PRO software at constant-volume adiabatic conditions. The premixed PODE$_1$/air charge was allowed to auto-ignite under predefined initial temperature ($T_{in}$), initial pressure ($P_{in}$) and equivalence ratio ($\varphi$). The following equations, designating the rate of change of instantaneous temperature (Eq. 1), pressure (Eq. 2), and the overall heat release (Eq. 3) inside the batch reactor, have been solved:

$$\frac{dT}{dt} = \left[R_u T \sum_i \dot{\omega}_i - \sum_i \left(\bar{h}_i \dot{\omega}_i\right)\right] / \sum_i \left[[X_i](\bar{c}_{p,i} - R_u)\right] \quad (1)$$

$$\frac{dP}{dt} = R_u T \sum_i \dot{\omega}_i + R_u \sum_i [X_i] \frac{dT}{dt} \quad (2)$$

$$\frac{dQ}{dt} = -V \sum_{i=1}^{N} (h_i \dot{\omega}_i) M_i \quad (3)$$

where $\dot{\omega}_i$, $\bar{h}_i$, $\bar{c}_{p,i}$, $[X_i]$ and $M_i$ are the production rates, specific molar enthalpies, constant-pressure specific heats, molar concentrations and molecular weights of species $i$, respectively; and $R_u$ and $V$ are the universal gas constant and the volume of batch reactor, respectively.

To elucidate the 3SHR macro-dynamics of PODE$_1$/air mixtures, an *initial-state sensitivity analysis* of two proposed sets of global (i.e., macro) HRR parameters: (1) the max/min values (according to stage: either 1st, 2nd or final; defined by $n$) (set #1), and (2) the in-between time-intervals (set #2), has been conducted (Table 1, Fig. 1). For these tasks, two PODE$_1$ mechanisms (by Jacobs et al. [10], Shrestha et al. [11]), found to most accurately represent lean PODE$_1$-AI [9], have been utilized. In addition, Zhang et al. [12] n-heptane mechanism was utilized for comparison purposes.

Table 1: Set matrix of proposed raw and normalized numerical PODE$_1$ 3SHR characteristics

| | Set # | Utilized profile | Derived raw characteristics | Rate of change with $T_{in}$* |
|---|---|---|---|---|
| *Max/min HRR values and time-points* | 1 | *HRR(t)* | $HRR^n_{\substack{min \\ max}}$, $\tau^n_{\substack{min \\ max}}$ | $HRR^{n'}_{\substack{min \\ max}}$ , $\tau^{n'}_{\substack{min \\ max}}$ |
| *Time intervals between the max/min HRR* | 2 | | $\Delta t^n_{HRR_{max}}$, $\Delta t^n_{phase}$ | $\Delta t^{n'}_{HRR_{max}}$, $\Delta t^{n'}_{phase}$ |

Note: * $(\cdot)' = -d(\log(\cdot))/dT_{in}$;

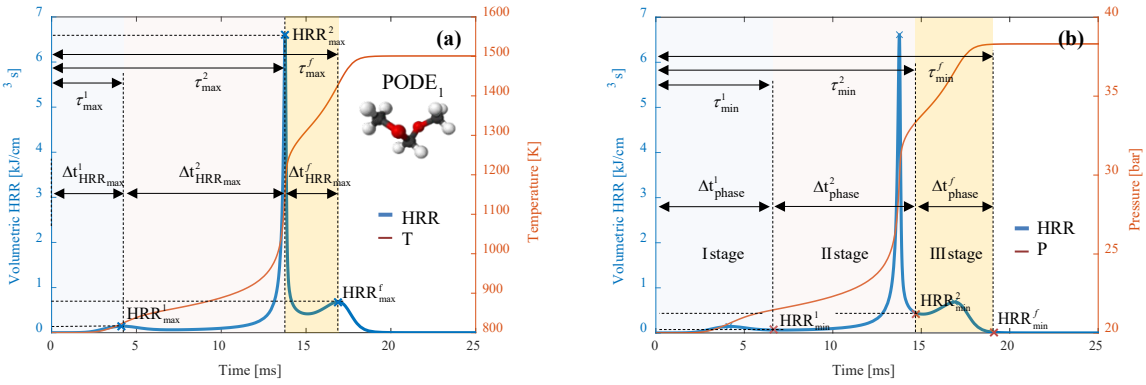


Fig. 1. Volumetric heat release rate (HRR), instantaneous temperature and pressure of PODE$_1$/air mixture at $T_{in}$ = 800 K, $P_{in}$ = 20 bar and $\varphi$ = 0.2, mechanism [10]. Max/min values of volumetric HRR: $HRR^n_{max,min}$ (a, b: x symbols), (2) corresponding time-points: $\tau^n_{max,min}$ (a, b), (3) intervals between $HRR^n_{max}$: $\Delta t^n_{HRR_{max}}$ (a), and (4) heat release phase times: $\Delta t^n_{phase}$ (b), $n$=1, 2, $f$ (1st ,2nd, final stage).

## 3. Results and discussion

The effect of $T_{in}$ appears to be significant on $\Delta t^{n}_{HRR_{max}}$, $\Delta t^{n}_{phase}$, and $HRR^{n}_{max}$ (or $HRR^{n}_{min}$), as shown in Fig. 2 (left). Briefly, the peak low-temperature heat release (LTHR) rate (Fig. 2a, ▫) (i) attains the highest values at the lower end of $T_{in}$ (i.e., 600 K), (ii) might be accompanied by second peak (e.g., 700 K), and (iii) overall decays with $T_{in}$ rise (↑), as the LTHR activity decreases (↓). Simultaneous patterns of *proximity*- and peak *amplitude*-↑ between and of, respectively, the former (Fig. 2a, ○) and latter (Fig. 2a, △) high-temperature heat-release (HTHR) stages are observed with $T_{in}$ ↑, until both merge (indicating a typical 2-stage ignition behavior of reactive fuels). Notably, Fig. 2b clearly shows that the third stage is associated with prolonged $CO_2$ and $H_2O$ formation (i.e., hydrogen-related, and CO-to-$CO_2$ chemistry).

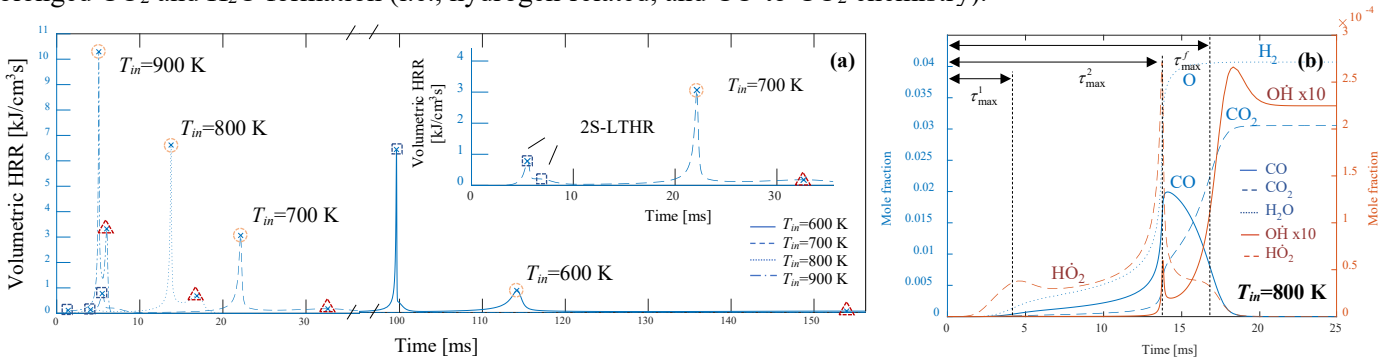


Fig. 2. Volumetric HRR (a) of PODE$_1$/air mixtures for [10] at $T_{in}$= 600-900 K, $P_{in}$ = 20 bar and $\varphi$ = 0.2 and speciation (b) at 800 K. Max/min vHRRs: $HRR^{n}_{max}$ (x symbols), corresp. time-points: $\tau^{n}_{max}$ ($n$=*1, 2, f*). $HRR^{1}_{max}$ denoted by ▫, $HRR^{2}_{max}$ by ○ and $HRR^{f}_{max}$ by △.

To further establish the effects of initial temperature $T_{in}$, pressure $P_{in}$ and $\varphi$ on the interrelationship patterns among the PODE$_1$ (and n-heptane) heat release prominences (*i*) the time periods (i.e., $\Delta t^{n}_{HRR_{max}}$), and (*ii*) logarithmic derivatives (with $T_{in}$) of corresponding-to-$HRR^{n}_{max}$ time-points (i.e., $\tau^{n'}_{max}$), were plotted. Fig. 3 depicts these values obtained with mechanisms [10], [11] (for PODE$_1$: a, b) and [12] (for n-heptane: c).

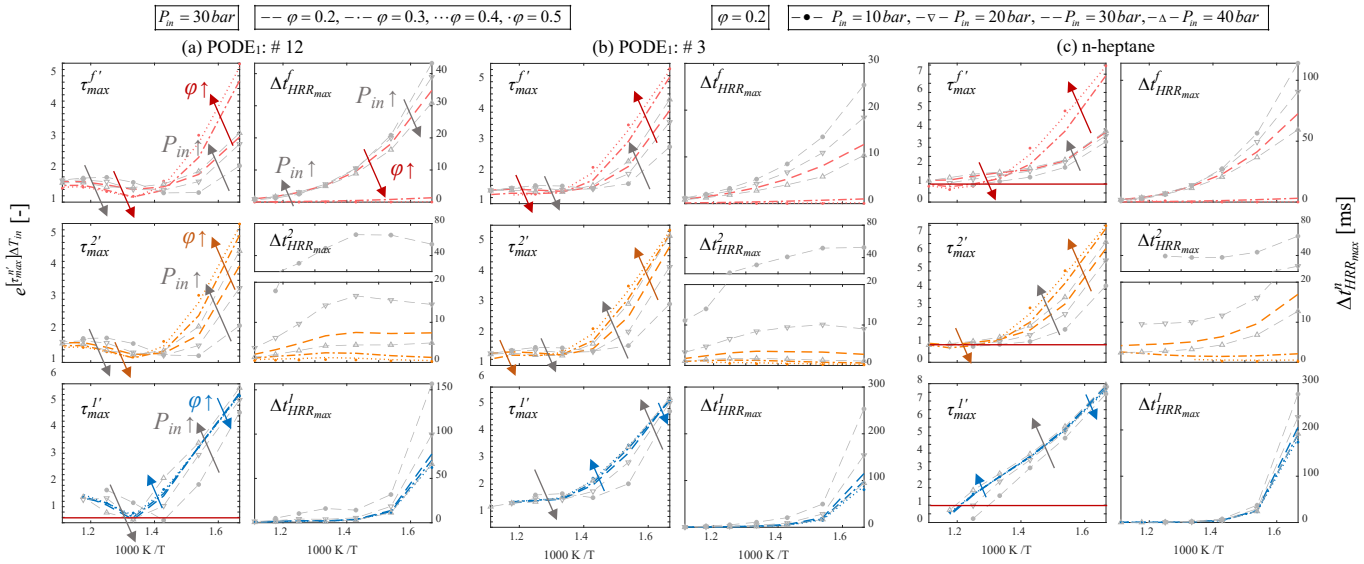


Fig. 3 $T_{in}$, $P_{in}$ and $\varphi$ effects on decrease rate of $\tau^{n}_{max}$ with $T_{in}$ (left columns: a, b, c) and $\Delta t^{n}_{HRR_{max}}$ (right columns: a, b, c) for PODE$_1$/air mixtures, mechanisms [10] (a), [11] (b) and of n-heptane/air mixtures [12] (c); for $\varphi$=0.2-0.5, $P_{in}$ = 30 bar and $T_{in}$ = 600-900 K (bold: red, orange, blue lines) and $\varphi$ = 0.2, $P_{in}$ = 10-40 bar and $T_{in}$ = 600-900 K (dotted: gray lines).

It is clear from Fig. 3 (right columns) that $\varphi$ has a strong effect on promoting the 3SHR phenomenon initially at any of examined $T_{in}$ and $P_{in}$ (i.e., simultaneous $\Delta t^{n=1,2,f}_{HRR_{max}}$ occurrence). The highest $\Delta t^{f}_{HRR_{max}}$ intervals (i.e., the 3rd-stage), obtained at $\varphi$ = 0.2 for both fuels, decay with $\varphi \uparrow$ as expected (top sub-figures, red lines). $P_{in} \uparrow$ effect on $\Delta t^{f}_{HRR_{max}}$ periods is oppositely altered with $T_{in} \uparrow$ (top sub-figures, gray lines), favoring $H_2O$ over $CO_2$ formation chemistry with $P_{in} \uparrow$ and $T_{in} \uparrow$, thus resulting in prolonged 3rd-stage interval.

Sensitivity analysis of $\tau^{2,f'}_{max}$ (Fig. 3, left columns) shows that $\varphi \uparrow$ and $P_{in} \uparrow$ effects are oppositely altered at certain $T_{in,}$ preserving the direction of alteration. One can clearly notice that for $PODE_1$ no $\tau^{2,f'}_{max}$ values below 1 are present (i.e., lack of negative temperature coefficient (NTC) behavior), contrary to n-heptane. $\tau^{1'}_{max}$ perturbation shows that both fuels respond with oppositely altered direction as $\varphi \uparrow$, however with $P_{in} \uparrow$ the direction is preserved for n-heptane. Moreover, n-heptane shows close to linear slopes of $\tau^{1'}_{max}$ with $T_{in} \uparrow$, contrary to $PODE_1$. Interestingly, $\Delta t^{2}_{HRR_{max}}$ profiles (affected by $\tau^{1,2'}_{max}$ rates) exhibit a different behavior among the fuels with $T_{in} \uparrow$. For $PODE_1$, $\Delta t^{2}_{HRR_{max}}$ tend to execute a *negative parabolic* profile, with the peak-value-shift to a higher $T_{in}$ as $\varphi \uparrow$. Contrary, for n-heptane $\Delta t^{2}_{HRR_{max}}$ *either decay* or show *a positive parabolic* profile, with the min-value-shift to a lower $T_{in}$ as $\varphi \uparrow$. The differences are linked to dissimilar NTC behavior of both fuels.

## 4. Conclusions

The current paper presents initial numerical insights into macro-dynamics of *three-stage heat release phenomenon* of $PODE_1$/air propellant, subjected to ultra-lean spontaneous auto-ignition at moderate pressures and low-to-intermediate temperatures (i.e., $T_{in}$=600-900 K, $P_{in}$=10-40 bar, and $\varphi$ = 0.1-0.5). *The initial-state sensitivity analysis* of the heat release rate characteristic parameters (i.e., $HRR^{n}_{max}$ and $\Delta t^{n}_{HRR_{max}}$) leads to the following conclusions:

- The peak LTHR rate (i) reaches the highest value at the lower end of $T_{in}$ (i.e., 600 K), (ii) might be accompanied by the second peak, and (iii) overall decays with $T_{in}$ rise, as the LTHR activity reduces.
- Simultaneous patterns of *proximity- and peak amplitude-rise* between and of, respectively, the former and latter HTHR stages are observed with $T_{in}$ rise, until both merge (depicting a typical 2-stage heat release pattern).
- $\varphi$ and $T_{in}$ have a strong effect on promoting 3SHR phenomenon, both reduce $\Delta t^{f}_{HRR_{max}}$ values if increased.
- $P_{in}$ rise exhibits contrary effect on $\Delta t^{f}_{HRR_{max}}$ with $T_{in}$ rise, slightly favoring $H_2O$ over $CO_2$ formation chemistry, resulting in prolonged 3rd-stage interval.
- $\Delta t^{2}_{HRR_{max}}$ profiles of $PODE_1$ and n-heptane fuels show *opposite trends* as $T_{in}$ rises: the former shows negative and the latter positive parabolic $\Delta t^{2}_{HRR_{max}}(T_{in})$ profiles, affected by differences in NTC behavior of compared fuels.

Further research steps comprise a broader macro-dynamic and thermo-chemical (i.e., micro-dynamic) analysis of 3SHR-$PODE_1$ phenomenon to comprehensively elucidate its effect on potential lean combustion modes.


## Acknowledgements

The authors gratefully acknowledge the financial support of the Israel Science Foundation (grant 2054/17).


## References


[1] Deutz S, Bongartz D, Heuser B, Kätelhön A, Schulze Langenhorst L, Omari A, Walters M, Klankermayer J, Leitner W, Mitsos A, Pischinger S, Bardow A. Cleaner production of cleaner fuels: wind-to-wheel – environmental assessment of CO2-based oxymethylene ether as a drop-in fuel. Energy Environ Sci 2018;11:331–43. https://doi.org/10.1039/C7EE01657C.

[2] Sun R, Delidovich I, Palkovits R. Dimethoxymethane as a Cleaner Synthetic Fuel: Synthetic Methods, Catalysts, and Reaction Mechanism. ACS Catal 2019;9:1298–318. https://doi.org/10.1021/acscatal.8b04441.

[3] Hank C, Lazar L, Mantei F, Ouda M, White RJ, Smolinka T, Schaadt A, Hebling C, Henning H. Comparative well-to-wheel life cycle assessment of OME3-5 synfuel production via the power-to-liquid pathway. Sustain Energy Fuels 2019;3:3219–33. https://doi.org/10.1039/c9se00658c.

[4] Ren Y, Huang Z, Miao H, Di Y, Jiang D, Zeng K, Liu B, Wang X. Combustion and emissions of a DI diesel engine fuelled with diesel-oxygenate blends. Fuel 2008;87:2691–7. https://doi.org/https://doi.org/10.1016/j.fuel.2008.02.017.
[5] Liu H, Wang Z, Wang J, He X, Zheng Y, Tang Q, Wang J. Performance, combustion and emission characteristics of a diesel engine fueled with polyoxymethylene dimethyl ethers (PODE3-4)/ diesel blends. Energy 2015;88:793–800. https://doi.org/10.1016/j.energy.2015.05.088.
[6] García A, Monsalve-Serrano J, Villalta D, Fogué-Robles Á. Evaluating OMEx combustion towards stoichiometric conditions in a compression ignition engine. Fuel 2021;303:121273. https://doi.org/10.1016/J.FUEL.2021.121273.
[7] Saxena S, Bedoya ID. Fundamental phenomena affecting low temperature combustion and HCCI engines, high load limits and strategies for extending these limits. Prog Energy Combust Sci 2013;39:457–88. https://doi.org/10.1016/j.pecs.2013.05.002.
[8] Eyal A, Thawko A, Baibikov V, Tartakovsky L. Performance and pollutant emission of the reforming-controlled compression ignition engine – Experimental study. Energy Convers Manag 2021;237:114126. https://doi.org/10.1016/J.ENCONMAN.2021.114126.
[9] Buntin D, Tartakovsky L. Heat release peculiarities of polyoxymethylene dimethyl ether 1 – Part I: Effect of initial thermochemical conditions. Fuel 2022;321:124007. https://doi.org/https://doi.org/10.1016/j.fuel.2022.124007.
[10] Jacobs S, Döntgen M, Alquaity ABS, Kopp WA, Kröger LC, Burke U, Pitsch H, Leonhard K, Curran H, Heufer K. Detailed kinetic modeling of dimethoxymethane. Part II: Experimental and theoretical study of the kinetics and reaction mechanism. Combust Flame 2019;205:522–33. https://doi.org/10.1016/j.combustflame.2018.12.026.
[11] Shrestha KP, Eckart S, Elbaz AM, Giri BR, Fritsche C, Seidel L, Roberts W, Krause H, Mauss F. A comprehensive kinetic model for dimethyl ether and dimethoxymethane oxidation and NOx interaction utilizing experimental laminar flame speed measurements at elevated pressure and temperature. Combust Flame 2020;218:57–74. https://doi.org/10.1016/j.combustflame.2020.04.016.
[12] Zhang K, Banyon C, Bugler J, Curran HJ, Rodriguez A, Herbinet O, Battin-Leclerc F, B'Chir C, Heufer K. An updated experimental and kinetic modeling study of n-heptane oxidation. Combust Flame 2016;172:116–35. https://doi.org/https://doi.org/10.1016/j.combustflame.2016.06.028.